LA-UR-16-27252

Approved for public release; distribution is unlimited.

Title:	Analysis of the LSC microbunching instability in MaRIE linac reference design
Author(s):	Yampolsky, Nikolai
Intended for:	Report
Issued:	2016-09-22

Analysis of the LSC microbunching instability in MaRIE linac reference design

Nikolai Yampolsky
Los Alamos National Laboratory, Los Alamos, New Mexico, 87545, USA
(Dated: April 15, 2016)

I. INTRODUCTION

In this report we estimate the effect of the microbunching instability in the MaRIE XFEL linac. The reference design for the linac is described in a separate report [1]. The parameters of the L1, L2, and L3 linacs as well as BC1 and BC2 bunch compressors were the same as in the referenced report. The beam dynamics was assumed to be linear along the accelerator (which is a reasonable assumption for estimating the effect of the microbunching instability). The parameters of the bunch also match the parameters described in [1]. Additionally it was assumed that the beam radius is equal to $R = 100\mu m$ and does not change along linac. This assumption needs to be revisited at later studies.

The beam dynamics during acceleration was accounted in the matrix formalism using a Matlab code. The input parameters for the linacs are: RF peak gradient, RF frequency, RF phase, linac length, and initial beam energy. The energy gain and the imposed chirp are calculated based on the RF parameters self-consistently. The bunch compressors are accounted in the matrix formalism as well. Each chicane is characterized by the beam energy and the R_{56} matrix element. It was confirmed that the linac and beam parameters described in [1] provide two-stage bunch compression with compression ratios of 10 and 20 resulting in the bunch of 3kA peak current.

II. LSC MICROBUNCHING GAIN

We begin our analysis with finding the gain for the microbunching instability. The analysis was done using the formalism developed in Ref. [2].

First, it was assumed that the electron bunch has modulation of the distribution function at a single longitudinal harmonic $f(z,p_z) = f_0(z,p_z)(1+b_0\exp(ikz))$. As shown in [2], the dynamics of modulated beams can be conveniently described in the Fourier space. For that one needs to find the Fourier transform of the distribution function which we call "spectral distribution function"(2D distribution function is sufficient for tracking the longitudinal dynamics), $f_{\mathbf{k}}(k_z,k_{p_z}) = (2\pi)^{-2}\int f(z,p_z)e^{-ik_z z - ik_{p_z}p_z}dzdp_z$. Longitudinal modulation of the bunch density (so as current) translates a single harmonic of the spectral distribution function at $\mathbf{k} = (k,0)^T$. The problem of calculating the LSC microbunching gain reduces to the problem of tracking the content of the spectral distribution function.

The evolution of modulation can be tracked through tracking the change of the 2D modulation wavevector. There are two type of elements in linac architecture: linacs which accelerate the beam and chicanes which provide compression. The linac section accelerates the beam, imposes energy chirp, and imposes sinusoidal modulation due to LSC. LSC energy modulation commutes with imposing energy chirp (the order of the energy change by two mechanisms for each particle does not matter). That allows us to split the individual particle motion in linac and accounting for collective LSC effect. In our analysis we can impose energy modulation due to LSC first and then account for linear changes to the distribution function due to off-crest acceleration. LSC imposes sinusoidal energy variation along the bunch which is proportional to the LSC impedance [3]. This sinusoidal in space energy modulation broadens the spectral distribution function along k_{p_z} as described in Sec. IIIB of Ref.[2]. Imposing the chirp on the beam and passing the beam through the chicane results in the linear change for the harmonic wavevector as $\mathbf{k} = R^{-T}\mathbf{k}_0$ [2].

We have knowledge about the dynamics of the spectral distribution function at each stage along linac and now we can compute the LSC microbunching gain. The microbunching instability results in the increased current modulation after the linac+BC section. The current modulation corresponds to the spatial modulation wavevector $\mathbf{k}_f = (k_f, 0)$. We can track the dynamics of this wavevector backwards along the accelerator through linear transform and find the modulation wavevector which transforms into current modulation after chirping and compression $\mathbf{k}_{LSC} = (R_{linac}R_{BC})^T\mathbf{k}_f$. The spatial z-component of the $\mathbf{k}_{LSC}$ should be the same as wavenumber of the imposed modulation, which gives us $k_f = k/(1+hR_{56})$. That allows one to find the k_{p_z} component of the 2D spectral distribution function which will be translated into current modulation after beam chirping and compression. The amplitude of the spectral distribution funtion at this wavevector will be bunching factor after the compressor. We find this amplitude following the analytics described in Ref. [2] as $f_{\mathbf{k}}(k_{p_z}) \propto J_1(|k_{p_z}(\delta p_z)_{LSC}|)$. The ratio of the bunching factor after the bunch compressor and before the linac is the gain G for the LSC microbunching instability. The second linac + bunch compression section can be analyzed in the same way. The gain for the 2 bunch compression stages is shown in Fig. 1. The gain is expected to be the largest for initial current modulations at the wavelengths of about $150\mu m$.

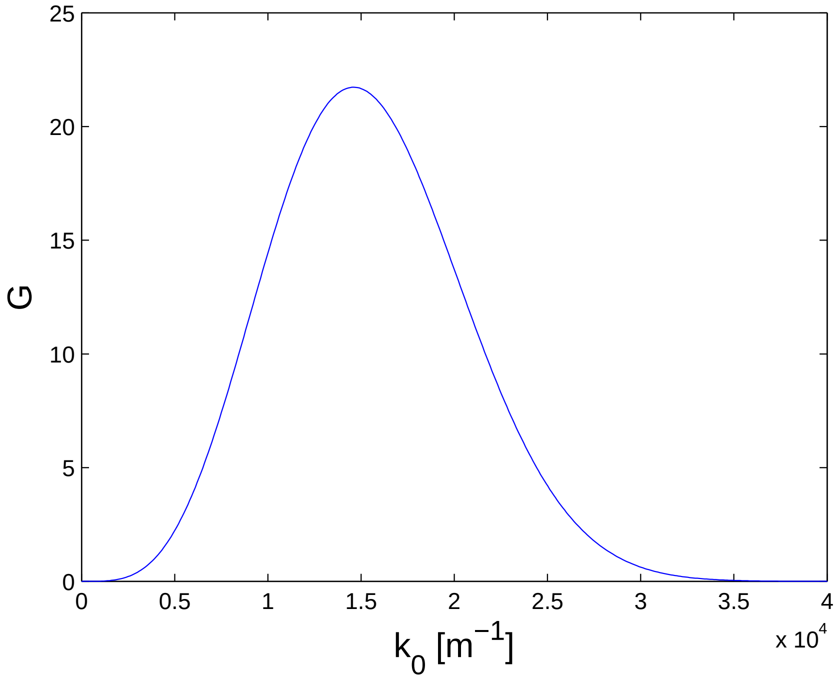

FIG. 1: Gain for the LSC microbunching instability after two-stage compression.

The results of this analysis were compared with the results presented in Ref. [3] (that approach was used by Quinn Marksteiner in his analysis of the microbunching instability). The single stage compression gain curves generated by these two approaches are identical. It is not surprising since the physics in those approaches is the same. The only differences in approaches is the intermediate math. It was also verified that the analytical expression for a single compressor microbunching instability gain resulted from the analysis described above agrees with the one reported in Ref. [3]. The full microbunching gain after the second bunch compressor are consistent between two approaches. There is a small difference on the order of several percent which can be explained by using slightly different level of accuracy in derivations and high sensitivity of the linac design vs. the input parameters.

III. LASER HEATER

The analysis for the growth of the microbunching instability can be expanded to estimate the growth of the rms energy spread in the beam. We assume that the most energy modulation growth occurs in L3 linac where the current modulation is the largest (this assumption is not necessarily correct since the LSC fields are larger at lower energy so the increase in rms energy spread in L2 or L1 may be significant). The spectral distribution current results in the electric field as

$$E_k(k) = Z(k)I_k(k), \qquad I_k(k) = \frac{1}{2\pi}\int I(z)e^{-ikz}dz. \tag{1}$$

The LSC-induced electric field results in the change of the particles' energy. The amplitude of the spectral current distribution is increased compared to the shot noise level proportionally to the microbunching instability gain $G(k)$. That allows one to find the spatial distribution of particles' energy along the bunch $\gamma(z)$ and calculate its average

$$\overline{|\delta\gamma(z)|^2} = \frac{1}{L}\left(\frac{e}{mc^2}\right)^2\int dz\int G(k_1)Z(k_1,s_1)I_k(k_1)G^*(k_2)Z^*(k_2,s_2)I_k^*(k_2)e^{i(k_1-k_2)z}dk_1dk_2ds_1ds_2 = \tag{2}$$

$$= \frac{1}{L}\left(\frac{e}{mc^2}\right)^2\int G(k_1)Z(k_1,s_1)I_k(k_1)G^*(k_2)Z^*(k_2,s_2)I_k^*(k_2)2\pi\delta(k_1-k_2)dk_1dk_2ds_1ds_2 = \tag{3}$$

$$= \frac{2\pi}{L}\left(\frac{e}{mc^2}\right)^2\int |G(k)I_k(k)\int Z(k,s)ds|^2dk \tag{4}$$

The rms energy variation should be averaged over various random realizations. We assume that the original current distribution is determined by the random shot noise.

$$< |I_k(k)|^2 > \ = \ \left(\frac{1}{2\pi}\right)^2 \left\langle \left| \int I(z) e^{-ikz} dz \right|^2 \right\rangle = \left(\frac{ec}{2\pi}\right)^2 \left\langle \left| \int \sum_n \delta(z - z_n) e^{-ikz} dz \right|^2 \right\rangle = \tag{5}$$

$$= \left(\frac{ec}{2\pi}\right)^2 \left\langle \left| \sum_n e^{-ikz_n} \right|^2 \right\rangle = \left(\frac{ec}{2\pi}\right)^2 \left\langle \sum_{n,m} e^{-ik(z_n - z_m)} \right\rangle = N \left(\frac{ec}{2\pi}\right)^2. \tag{6}$$

This averaged over multiple random distributions current spectrum can be used to find the final rms energy slice energy change in the bunch (assuming that the current varies along the bunch on a larger scale than the characteristic wavelength for the microbunching instability).

$$\left\langle \overline{|\delta\gamma(z)|^2} \right\rangle = \frac{I}{2\pi ec} \frac{N}{N_{macro}} \left(\frac{e^2}{mc}\right)^2 \int \left| G(k) \int Z(k, s) ds \right|^2 dk. \tag{7}$$

Here we have introduced the parameter N_{macro}. It reflects the fact that the noise level in current distribution can be higher compared to the random shot noise. This parameter is useful while comparing results of numerical simulations with predictions of this report. The number of particles used in particle pushing codes like ELEGANT is typically much smaller than in a real bunch. As a result, the current noise level in simulated bunches is higher than in real life bunches and the increased energy spread can be expected in simulations.

The expression for the LSC-induced heating was compared with results obtained by Quinn Marksteiner. The scaling is the same but two expressions have different numerical factors. Elimination of discrepancy and benchmarking results with numerical simulations will be performed in near future.

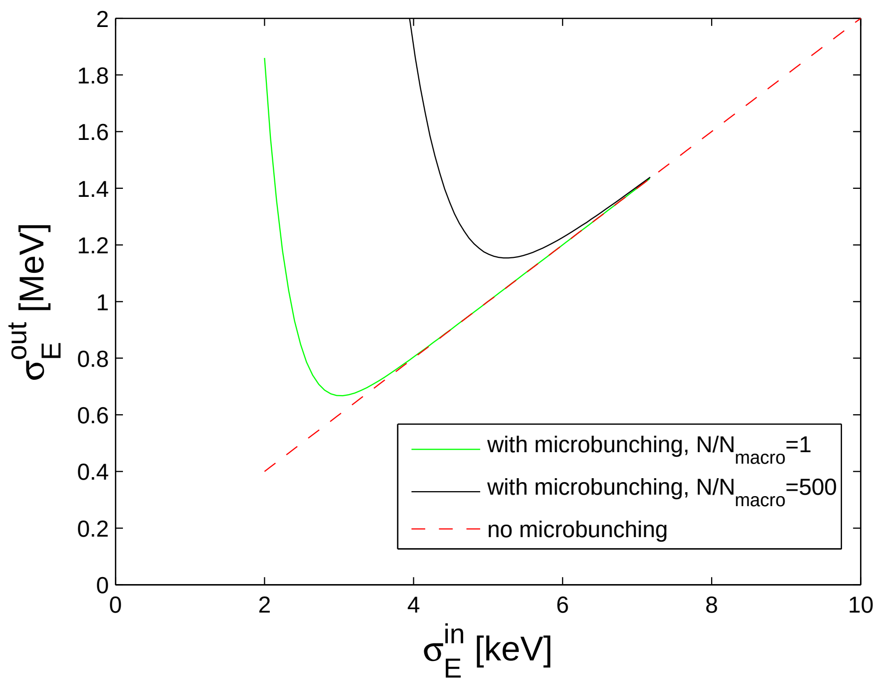

FIG. 2: The output bunch slice energy spread vs. the initial energy spread.

The microbunching instability followed by the energy modulation in L3 results in the increased rms slice energy spread of the bunch as $(\delta\gamma)^2 = (\delta\gamma_{LSC})^2 + (\delta\gamma_{intrinsic})^2$. The larger initial energy spread reduces the microbunching instability gain and the associated energy modulation. As a result, the resulting energy spread at the end of L3 is dominated by the LSC microbunching instability at low initial energy spread and it is dominated by the intrinsic energy spread when it is large enough. This effect is demonstrated in Fig. 2 which shows the estimated slice energy spread in the bunch after L3 when the microbunching instability is taken into account. The artificial instantaneous energy chirp was provided to the beam at different initial energy spread to get the same compression ratios as in reference design at 5keV.

Fig. 2 shows that the optimal pre-compressed energy spread should be about 5.2keV. This number can be used as an estimate for the anticipated laser heater parameters. This optimal initial energy spread is consistent with the MaRIE reference design point used in Ref. [1] which is 5keV ($N/N_{macro} = 500$ is used to match numerical simulations). More accurate estimate for the laser heater parameters can be done in future to account for beam focusing and energy spread growth after BC1.

[1] J. Lewellen, "Compressor trade study". MaRIE work package report e-mailed to B. Carlsten on 1/13/16.
[2] N. A. Yampolsky, "Description of modulated beam dynamics", http://arxiv.org/abs/1112.0553 (2011).
[3] Z. Huang, M. Borland, P. Emma, J. Wu, C. Limborg, G. Stupakov, and J. Welch, "Suppression of microbunching instability in the linac coherent light source", Phys. Rev. ST-AB **7**, 074401 (2004).